Hybrid functionals with local range separation

Aliaksandr V. Krukau,[1] Gustavo E. Scuseria,[1,a)] John P. Perdew,[2] and Andreas Savin[3]
[1]*Department of Chemistry, Rice University, Houston, Texas 77005-1892, USA*
[2]*Department of Physics and Quantum Theory Group, Tulane University, New Orleans, Louisiana 70118, USA*
[3]*Laboratoire de Chimie Théorique, CNRS, Universite Pierre et Marie Curie, 4 Place Jussieu, F-75252 Paris, France*

(Received 23 June 2008; accepted 14 August 2008; published online 23 September 2008)

Range-separated (screened) hybrid functionals provide a powerful strategy for incorporating nonlocal exact (Hartree–Fock-type) exchange into density functional theory. Existing implementations of range separation use a fixed system-independent screening parameter. Here, we propose a novel method that uses a position-dependent screening *function*. These locally range-separated hybrids add substantial flexibility for describing diverse electronic structures and satisfy a high-density scaling constraint better than the fixed screening approximation does. © *2008 American Institute of Physics*. [DOI: 10.1063/1.2978377]

I. INTRODUCTION

The concept of screening the interelectronic Coulomb interaction has a long history in condensed matter physics.[1] In many-body theory, the interelectronic interaction is modified by a microscopic frequency-dependent dielectric constant.[2] In the context of density functional theory (DFT), screened Hartree–Fock (HF) type exchange has been combined with the local spin-density approximation (LSDA) providing successful approximations for band gaps of semiconductors.[3,4] In finite systems, the concept of "range separation" was introduced in order to combine DFT and wavefunction theory.[5–7] In this approach, the Coulomb interaction is split into short-range (SR) and long-range (LR) components:

$$\frac{1}{u} = \underbrace{\frac{1-\mathrm{erf}(\omega u)}{u}}_{\mathrm{SR}} + \underbrace{\frac{\mathrm{erf}(\omega u)}{u}}_{\mathrm{LR}}, \tag{1}$$

where the screening parameter ω defines the range separation and u represents the interelectronic distance. The short-range part of the exchange-correlation energy is then treated by semilocal approximations from DFT, whereas the long-range part is calculated from wavefunctions, specifically the HF theory at the simplest level. When $\omega \to \infty$, all of the Coulomb interactions in the exchange-correlation energy are treated as LR; when $\omega \to 0$, all of them are treated as SR.

Range separation provides a powerful tool for combining DFT with wavefunction theory in practical applications where the decay of the exchange-correlation potential is important[8,9] or where static correlation (a LR effect) plays a crucial role.[10] For instance, the LC-ωPBE functional, which combines LR HF with SR PBE exchange, yields accurate enthalpies of formation and barrier heights simultaneously (see Refs. 9 and 11). As discussed in Ref. 12, HF is exact at LR for atoms and molecules but not for extended metals.

In a seemingly opposing approach having solid-state systems in mind, Heyd *et al.* proposed a screened hybrid functional known as HSE (Refs. 13–15) that incorporates SR HF-type exchange but neglects its LR portion, which is problematic in narrow band gap semiconductors and metals.[16,17] HSE has been very successful in predicting a wide range of molecular and solid-state properties.[18–23] These contrary views (keeping HF exchange for LR in LC-ωPBE versus SR in HSE) can be reconciled in a three-range hybrid which uses HF exchange only in the middle range.[24] The HISS functional combines the attractive features of both HSE and LC-ωPBE.[25]

Range-separated hybrid functionals offer a promising route for the construction of accurate density functionals. However, most previous implementations of range separation use a universal system-independent screening parameter. It seems obvious that such an approach, despite its success, will have limitations. It has been argued that the screening parameter should rather be system dependent.[3,6,26,27] In this paper, we describe an even more general approach. In the homogeneous electron gas, the size of the exchange hole measured, e.g., by the point where its first node appears, varies with the density of the gas. Therefore, it seems evident that the separation between the SR and LR interactions for an inhomogeneous system should depend on the local density. Here, we propose an approximation that uses a position-dependent screening function $\omega(\mathbf{r})$ defining a *local* range separation (LRS) for mixing exact (HF-type) and LSDA exchange. Our approach is presented in detail below.

II. THEORY

A. Physical idea

We propose the following form for the exchange-correlation energy of a spin-unpolarized density:

a)Electronic mail: guscus@rice.edu.

$$E_{\mathrm{xc}}^{\mathrm{LRS}\text{-}\omega\mathrm{LSDA}} = \int [e_x^{\mathrm{LSDA,SR}}(\mathbf{r},\omega(\mathbf{r})) + e_x^{\mathrm{HF,LR}}(\mathbf{r},\omega(\mathbf{r}))]d\mathbf{r} + E_c^{\mathrm{LSDA}}. \quad (2)$$

We will refer to this locally range-separated functional as LRS-ωLSDA. For simplicity of notation, we do not include spin indices in this paper. Equation (2) is readily extended to spin-polarized systems using the spin-scaling relationship[28] for the exchange energy [with an $\omega(\mathbf{r})$ for each spin component] and the standard generalization for correlation. When ω is universal and position independent, this functional reduces to LR corrected LSDA,[9,29] which we will here refer to as LC-ωLSDA. Note that in Ref. 29, this functional is denoted RSHXLDA. Toulouse *et al.*[30] suggested using a local screening parameter ω for DFT correlation. We here explore a LRS approach for exchange only; our aim is to combine it with LRS correlation at a later stage.

The realization and implementation of Eq. (2) is nontrivial. One should choose an appropriate screening function $\omega(\mathbf{r})$. There are several straightforward choices for the local screening parameter. In the homogeneous electron gas, the characteristic length is given by the Wigner–Seitz radius $r_s = (4\pi\rho/3)^{-1/3}$. The screening parameter has dimensions of inverse length, so a trivial selection would be $\omega(\mathbf{r}) \sim 1/r_s$.[30,31] For inhomogeneous systems, the screening function can be approximated by a gradient expansion:

$$\omega(\mathbf{r}) = \frac{1}{r_s}(\alpha + \beta s + \gamma s^2 + \ldots), \quad (3)$$

where $s = |\nabla\rho|/(2k_F\rho)$ is the reduced gradient, $k_F = (3\pi^2\rho)^{1/3}$, and α, β, and γ are the parameters to be determined. In the high-density limit, these choices for $\omega(\mathbf{r})$ have a better scaling behavior than constant ω (see Appendix A).

B. Computational implementation

The SR component can be calculated as

$$e_x^{\mathrm{LSDA,SR}}(\mathbf{r},\omega(\mathbf{r})) = \frac{1}{2}\rho(\mathbf{r})\int_0^\infty h_x^{\mathrm{LSDA}}(\rho(\mathbf{r}),u)\frac{\mathrm{erfc}(\omega(\mathbf{r})u)}{u} \times 4\pi u^2 du, \quad (4)$$

where $h_x^{\mathrm{LSDA}}(\rho(\mathbf{r}),u)$ is the LSDA exchange hole and $\mathrm{erfc}(x) = 1 - \mathrm{erf}(x)$. This integral can be done analytically for any value of ω.[7,32] Note that even though Eq. (4) is not symmetric with respect to interchange of electrons, it does not violate symmetry invariance of the total exchange energy, as explained in Appendix B.

The LR part (in the conventional gauge[33]) is defined as

$$e_x^{\mathrm{HF,LR}}(\mathbf{r},\omega(\mathbf{r})) = \sum_{\mu\nu}\phi_\mu(\mathbf{r})\phi_\nu(\mathbf{r})X_{\mu\nu}^{\mathrm{LR}}(\mathbf{r},\omega(\mathbf{r})), \quad (5)$$

where ϕ_μ and ϕ_ν are the atomic orbitals (AOs) and

$$X_{\mu\nu}^{\mathrm{LR}}(\mathbf{r},\omega(\mathbf{r})) = -\frac{1}{2}\sum_{\lambda\sigma}P_{\mu\lambda}P_{\nu\sigma}V_{\lambda\sigma}^{\mathrm{LR}}(\mathbf{r},\omega(\mathbf{r})), \quad (6)$$

where $\mathbf{P}$ is the density matrix and $V_{\lambda\sigma}^{\mathrm{LR}}$ are the Coulomb-type electrostatic integrals (ESIs):

$$V_{\lambda\sigma}^{\mathrm{LR}}(\mathbf{r},\omega(\mathbf{r})) = \int \phi_\lambda(\mathbf{r}')\phi_\sigma(\mathbf{r}')\frac{\mathrm{erf}[\omega(\mathbf{r})|\mathbf{r}-\mathbf{r}'|]}{|\mathbf{r}-\mathbf{r}'|}d\mathbf{r}'. \quad (7)$$

These integrals can be done analytically for any $\omega(\mathbf{r})$ (see Appendix C). The LR Fock exchange matrix may be evaluated from Eq. (7) as

$$K_{\mu\nu}^{\mathrm{LR}}(\omega(\mathbf{r})) = -\sum_{\lambda\sigma}P_{\lambda\sigma}\int \phi_\mu(\mathbf{r})\phi_\lambda(\mathbf{r})V_{\sigma\nu}^{\mathrm{LR}}(\mathbf{r},\omega(\mathbf{r}))d\mathbf{r} \quad (8)$$

and the LR exchange energy is evaluated as

$$E_x^{\mathrm{HF,LR}} = \int e_x^{\mathrm{HF,LR}}(\mathbf{r},\omega(\mathbf{r}))d\mathbf{r} = \frac{1}{2}\sum_{\mu\nu}K_{\mu\nu}^{\mathrm{LR}}(\omega(\mathbf{r}))P_{\mu\nu}. \quad (9)$$

Unfortunately, these expressions are computationally intractable as written. Given an arbitrary $\omega(\mathbf{r})$, the integral over $\mathbf{r}$ in Eq. (8) must be performed numerically. There are $\mathcal{O}(N_{\mathrm{AO}}^2)$ matrix elements of $V_{\sigma\nu}^{\mathrm{LR}}(\mathbf{r},\omega(\mathbf{r}))$ to be evaluated at each grid point $\mathbf{r}$, yielding a total computational cost $\mathcal{O}(N_{\mathrm{grid}}N_{\mathrm{AO}}^2)$. On the other hand, if $\omega(\mathbf{r})$ is constant, the integral over $\mathbf{r}$ in Eq. (8) can be performed analytically in a Gaussian basis set, leading to

$$K_{\mu\nu}^{\mathrm{LR}}(\omega) = -\sum_{\lambda\sigma}(\mu\lambda,\nu\sigma)_\omega P_{\lambda\sigma} \quad (10)$$

and

$$E_x^{\mathrm{HF,LR}} = \frac{1}{2}\sum_{\mu\nu\lambda\sigma}(\mu\lambda,\nu\sigma)_\omega P_{\mu\nu}P_{\lambda\sigma}, \quad (11)$$

where

$$(\mu\lambda,\nu\sigma)_\omega = \int\int \phi_\mu(\mathbf{r})\phi_\lambda(\mathbf{r})\frac{\mathrm{erf}(\omega|\mathbf{r}-\mathbf{r}'|)}{|\mathbf{r}-\mathbf{r}'|} \times \phi_\nu(\mathbf{r}')\phi_\sigma(\mathbf{r}')d\mathbf{r}d\mathbf{r}'. \quad (12)$$

Such analytic two-electron integrals are an essential part of Gaussian-orbital based electronic structure programs. For screened interactions, the integrals in Eq. (12) can be evaluated as a trivial modification of regular two-electron integrals.[7,34] While their computational scaling is formally $\mathcal{O}(N_{\mathrm{AO}}^4)$, they quickly reach their classical $\mathcal{O}(N_{\mathrm{AO}}^2)$ asymptote for moderate size systems,[35] and a variety of linear-scaling treatments have been developed for large systems.[36] Of course for $\omega \to \infty$, all these expressions recover their exact values for the bare unscreened interaction.

As explained in detail below, an approximation to the screened HF exchange energy density is needed for computational convenience. An alternative approach for calculating the HF exchange energy density is the method of Della Salla and Görling.[37] In this method, which we here extend for using with screened interactions, the expression for the HF exchange energy density is simplified by introducing a resolution of the identity (RI) in an auxiliary basis identical to the AO basis and leads to the following expansion:

$$e_x^{\mathrm{HF,LR}}(\mathbf{r},\omega) = \sum_{\mu\nu}\phi_\mu(\mathbf{r})\phi_\nu(\mathbf{r})Q_{\mu\nu}^{\mathrm{LR}}(\omega), \quad (13)$$

where

$$\mathbf{Q}^{\mathrm{LR}}(\omega) = \tfrac{1}{2}\mathbf{S}^{-1}\mathbf{K}^{\mathrm{LR}}(\omega)\mathbf{P} + \tfrac{1}{2}\mathbf{P}\mathbf{K}^{\mathrm{LR}}(\omega)\mathbf{S}^{-1}, \tag{14}$$

and $\mathbf{S}^{-1}$ is the inverse overlap matrix. Note the similarities between Eqs. (5) and (13). However, also note that while $\mathbf{X}$ depends on $\mathbf{r}$, $\mathbf{Q}$ is independent of it. The former is exact whereas the latter is approximate.

Given $\mathbf{Q}$, Eq. (13) can readily be evaluated at every grid point with minimal computational cost. While the orbital product $\phi_\mu(\mathbf{r})\phi_\nu(\mathbf{r})$ decays exponentially with increasing distance between AOs, the Coulomb-type ESIs of Eq. (7) do not decay as fast. Thus, for constant ω (including $\omega\to\infty$, i.e., the bare interaction), RI is usually preferred over ESIs for calculating $e_x^{\mathrm{HF,LR}}(\mathbf{r},\omega)$ because of its lower computational cost.[38] Note that an important savings consideration in RI is that for constant ω, $\mathbf{K}$ (needed for $\mathbf{Q}$) can be obtained analytically via modified two-electron integrals, Eq. (10).

For a local screening function $\omega(\mathbf{r})$, $\mathbf{K}$ can no longer be evaluated analytically and has to be done numerically via Eq. (8), which involves evaluation of ESIs, so the computational advantage of RI disappears. In summary, with LRS, both the RI and exact ESI procedures have similarly steep computational costs, requiring an $\mathcal{O}(N_{\mathrm{grid}}N_{\mathrm{AO}}^2)$ computational step that we wish to avoid. Therefore, we shall seek an alternative approximation for evaluating $e_x^{\mathrm{HF,LR}}(\mathbf{r},\omega(\mathbf{r}))$ whose computational cost is not much larger than evaluating the unscreened ($\omega\to\infty$) HF exchange energy density, which can be efficiently done via RI.

Let us recall that the TPSS exchange hole[39] was specifically constructed to reproduce the TPSS exchange energy density:

$$e_x^{\mathrm{TPSS}}(\mathbf{r}) = \frac{1}{2}\rho(\mathbf{r})\int_0^\infty \frac{h_x^{\mathrm{TPSS}}(\rho,|\nabla\rho|,\tau,e_x^{\mathrm{TPSS}},u)}{u}4\pi u^2 du, \tag{15}$$

where $h_x^{\mathrm{TPSS}}(\rho,|\nabla\rho|,\tau,e_x^{\mathrm{TPSS}},u)$ is the model TPSS exchange hole[39] and τ is the kinetic energy density. To achieve this goal, the TPSS hole expression has e_x^{TPSS} as an ingredient. We propose here to use the TPSS hole expression for reproducing the screened HF exchange energy density. We feed in the unscreened e_x^{HF} instead of e_x^{TPSS} in the above equation and integrate with the screened interaction to yield the following approximation:

$$e_x^{\mathrm{HF,LR}}(\mathbf{r},\omega(\mathbf{r})) \approx \frac{1}{2}\rho(\mathbf{r})\int_0^\infty h_x^{\mathrm{TPSS}}(\rho,|\nabla\rho|,\tau,e_x^{\mathrm{HF}},u) \times \frac{\mathrm{erf}(\omega(\mathbf{r})u)}{u}4\pi u^2 du. \tag{16}$$

For $\omega\to\infty$, Eq. (16) is exact. The accuracy of this approximation is examined in the next section. Note that the conventional gauge of the HF energy density e_x^{HF} in Eq. (5) differs slightly from the gauge of the TPSS energy density e_x^{TPSS}, as studied in Ref. 33, leading to a small error in Eq. (16) even when the integrated HF and TPSS exchange energies are equal for good reason. Because the TPSS exchange hole is based on the PBE hole model, the integral in Eq. (16) can be done (mostly) analytically, as shown in Refs. 13 and 14. This yields a procedure with rather moderate computational cost compared to the numerical integration alternatives via RI and ESIs discussed above. A recently redeveloped PBE hole model[40] can be extended to include the exchange energy density as an ingredient (resembling the TPSS hole) and still afford exact (as opposed to "mostly") analytic integration for screened interactions.

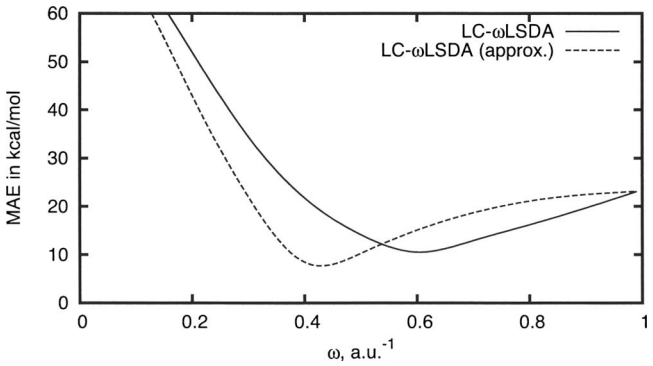

FIG. 1. MAEs for the standard enthalpies of formation of the AE6 set for exact and approximate LC-ωLSDA using Eq. (16) for $e_x^{\mathrm{HF,LR}}(\mathbf{r},\omega(\mathbf{r}))$.

On the ladder[41] of density functional approximations for the exchange-correlation energy, each rung represents the addition of a new ingredient: the local density, its gradient, the kinetic energy density, etc. The fourth or hyper-GGA (generalized gradient approximation) rung introduces the exact exchange energy density. From the perspective of ladder approximations and even though not explicit from the expressions in Eqs. (5)–(7), range-separated hybrids introduce further ingredients, minimally the spherically averaged exact exchange hole density $h_x^{\mathrm{ex}}([\rho];\mathbf{r},u)$, and thus stand at least slightly higher than the fourth rung. In our actual implementation of Eq. (2), by using Eq. (16), we are making a hyper-GGA approximation to a range-separated hybrid.

III. RESULTS AND DISCUSSION

We have implemented LRS-ωLSDA into the development version of the Gaussian suite of programs.[42] All benchmark calculations were performed non-self-consistently using LSDA orbitals. For LSDA correlation, we use the Perdew–Wang parametrization.[43] The unscreened HF exchange energy density, needed as an ingredient for Eq. (16), is calculated using the RI method [Eq. (13)].[37] This method works best with large and uncontracted basis sets, so we have used the uncontracted 6-311++G($3df,3pd$) basis set unless otherwise specified. When presenting our results, we employ the convention: deviation=theory−experiment. Unless specified otherwise, we use the equilibrium B3LYP/6-31G($2df,p$) geometries and zero-point energies for all species. Thermal corrections are calculated with a frequency scale factor of 0.9854.

The performance of our approximate expression for the locally screened LR HF exchange energy, Eq. (16), can be calibrated in a benchmark case where we know the correct answer. In Fig. 1 we plot mean absolute errors (MAE) in enthalpies of formation as a function of ω for LC-ωLSDA and the same functional evaluating the LR HF exchange energy density using the TPSS exchange hole approximation of Eq. (16) instead of the rigorous expression of Eq. (11). Re-

TABLE I. Deviation from the experiment of standard enthalpies of formation for position-dependent LC-ωLDA. AE6 test was used. All values are in kcal/mol.

Method	$\omega(\mathbf{r})$	η	MAE
LDA			77.7
LC-ωLDA	0.6		10.6
LRS-ωLDA	η/r_s	1	24.2
LRS-ωLDA	ηs	0.29	6.6
LRS-ωLDA	$\eta s^2/r_s$	0.3	5.4
LRS-ωLDA	$\eta\|\nabla\rho\|/\rho$	0.135	3.6
HF exch+LDA corr			50.8

sults presented in Fig. 1 are post-LSDA (i.e., done with LSDA orbitals) and we use the AE6 test set of standard enthalpies of formation.[44] This test set includes only six molecules, but it has been constructed to reproduce the errors of the much larger G3 set.[45]

The "exact" LC-ωLSDA in Fig. 1 shows the lowest MAE of 10.5 kcal/mol for $\omega=0.60$. Best results with the approximate LC-ωLSDA are achieved with $\omega=0.40$, where the MAE is 8.4 kcal/mol. Therefore, we conclude that Eq. (16) yields reasonably accurate results for thermochemistry, even though the optimal screening parameters are different. Note also that these optimal values would slightly change if obtained with self-consistent orbitals as opposed to the post-LSDA procedure used here.

In order to test the proposed LRS-ωLSDA approach, we use Eq. (3) for the local screening parameter. We have explored the parameter space for α, β, and γ in Eq. (3). Our current attempts indicate that optimal results are achieved with α, $\gamma\approx 0$. We can then rewrite Eq. (3) in terms of the density and its gradient:

$$\omega(\mathbf{r}) = \frac{\beta s}{r_s} = \frac{\eta|\nabla\rho|}{\rho}, \tag{17}$$

where $\eta=(18\pi)^{-1/3}\beta$. This choice of screening function was previously proposed by Toulouse *et al.*[30] In Table I, we present the results for the AE6 test set of standard enthalpies of formation with several versions of LRS-ωLSDA and related functionals. For each $\omega(\mathbf{r})$ approximation, we show the optimal value of the scaling parameter η and corresponding MAE. Note that LC-ωLSDA data in this and all subsequent tables are calculated with screening parameter $\omega=0.60$. The

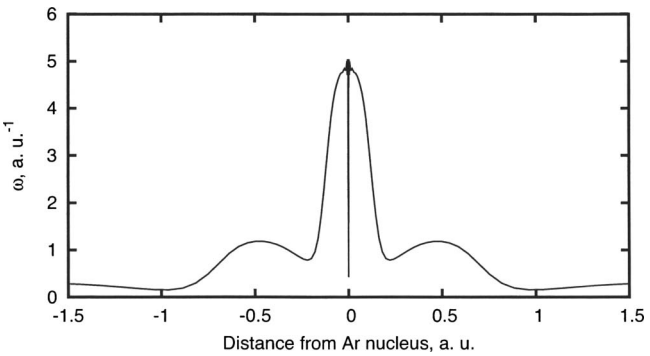

FIG. 2. Range separation function $\omega(\mathbf{r})$ in the argon atom, plotted as a function of the distance from nucleus.

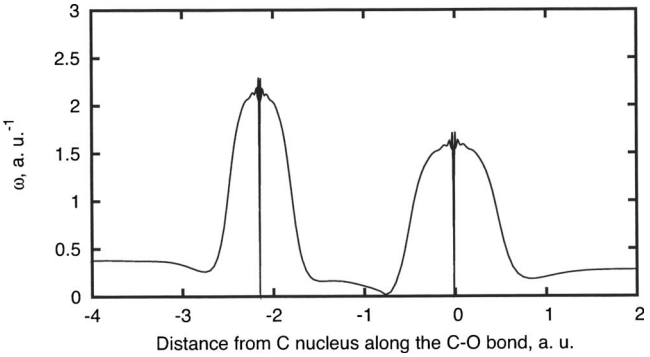

FIG. 3. Range separation function $\omega(\mathbf{r})$ for the majority-spin density, plotted along the bond axis of the CO molecule.

lowest MAE in Table I is achieved with $\omega(\mathbf{r})$ given by Eq. (17) and $\eta=0.135$.

It is interesting to note that the expression $|\nabla\rho|/\rho$ has been used as a "local band gap."[46] For the homogeneous electron gas, the local band gap reduces to zero, and there is no HF exchange in our functional. Moreover, in regions with strongly varying electronic density, $\omega(\mathbf{r})\to\infty$, so that HF exchange dominates. Both of these conditions have been proposed as constraints for hyper-GGAs, i.e., functionals that include the exact exchange energy density as an ingredient.[47] Also, $\eta|\nabla\rho|/\rho$ was used as a characteristic scale for density variations in the early GGA of Langreth and Mehl.[48] These authors settled on the value $\eta=0.15$ which is not far from our optimized $\eta=0.135$.

Plots of $|\nabla\rho|/\rho$ for atoms were presented several years ago in Refs. 49 and 50. Here, in Figs. 2 and 3, we present the plots of our screening function $\omega(\mathbf{r})$ in the Ar atom and the

TABLE II. Total non-relativistic energies of atoms (a.u.) with the incontracted UGBS basis set.

Atom	LSDA	LC-ωLSDA	LRS-ωLSDA	Exact[a]
H	−0.479	−0.516	−0.501	−0.500
He	−2.834	−2.925	−2.909	−2.904
Li	−7.343	−7.443	−7.467	−7.478
Be	−14.446	−14.560	−14.621	−14.667
B	−24.354	−24.493	−24.582	−24.654
C	−37.468	−37.636	−37.742	−37.845
N	−24.134	−54.332	−54.448	−54.589
O	−74.527	−74.757	−74.895	−75.067
F	−99.110	−99.368	−99.520	−99.734
Ne	−128.230	−128.511	−128.672	−128.938
Na	−161.44	−161.729	−161.931	−162.255
Mg	−199.135	−199.420	−199.664	−200.053
Al	−241.317	−241.609	−241.893	−242.346
Si	−288.216	−288.519	−288.834	−289.359
P	−340.000	−340.319	−340.657	−341.259
S	−396.737	−397.077	−397.439	−398.110
Cl	−459.662	−459.024	−459.402	−460.148
Ar	−525.940	−526.324	−526.714	−527.540
ME/$\bar{e}$[b]	0.064	0.040	0.026	
MAE/$\bar{e}$[c]	0.064	0.043	0.026	

[a]Reference 53.
[b]Mean error per electron.
[c]Mean absolute error per electron.

TABLE III. Deviations from experiment of standard enthalpies of formation ($\Delta_f H^o_{298}$) and barrier heights of chemical reactions computed with various methods using the uncontracted 6-311++G($3df,3pd$) basis set. All values are in kcal/mol.

	$\Delta_f H^o_{298}$ (kcal/mol)							
	G2 set		G3 set		HTBH38		NHTBH38	
Functional	ME	MAE	ME	MAE	ME	MAE	ME	MAE
LSDA	−83.0	83.0	−120.9	120.9	−17.9	17.9	−12.4	12.6
LC-ωLSDA	−2.0	10.5	−2.5	12.2	7.0	7.1	8.6	8.6
LRS-ωLSDA	−2.4	5.0	0.9	5.9	−5.4	5.5	−5.3	5.5

CO molecule, respectively. The screening function $\omega(\mathbf{r})$ has local maxima at nuclear positions, decreases in the valence region, and increases again in the density tail. Small oscillations around the nuclei are due to the use of Gaussian basis functions.

The asymptotic behavior of $|\nabla\rho|/\rho$ is well known. As $r\to\infty$, the density decays like[51] $Ar^{2\beta}\exp(-2\alpha r)$, where (in a.u.) $\alpha=(-2\epsilon_{\mathrm{HOMO}})^{1/2}$ and ϵ_{HOMO} is the highest-occupied (or partly occupied) orbital energy, and $\beta=1/\alpha-1$ for a neutral system. (For the hydrogen atom, for example, $\alpha=1$ and $\beta=0$.) Thus, $|\nabla\rho|/\rho\to 2\alpha$.

Based on the results of Table I, we decided to study LRS-ωLSDA with $\omega=0.135|\nabla\rho|/\rho$ in more details. In Table II, we present the calculated atomic energies for H to Ar with the large UGBS basis set.[52] We compare LSDA, LC-ωLSDA, and LRS-ωLSDA with accurate nonrelativistic energies.[53] LRS-ωLSDA has lower mean error per electron than either LSDA or LC-ωLSDA.

To assess the performance of LRS-ωLSDA for enthalpies of formation in more general cases, we have used the G3/99 test set of 223 molecules[45] and its smaller subset G2/97 of 148 molecules.[54] Note that we discarded the NO molecule from both benchmark sets because of convergence problems with LSDA. The results are presented in Table III. LC-ωLSDA dramatically reduces MAE for the G3 test set in comparison with LSDA. However, even better results are achieved with LRS-ωLSDA that yields MAE(G3) of 5.9 kcal/mol. For thermochemistry, LRS-ωLSDA is competitive with many common hybrid functionals.[55] For comparison purposes, the popular B3LYP functional yields MAEs of 3.1 and 4.9 kcal/mol for the G2 and G3 sets, respectively.[55]

Table III also shows the benchmark results for reaction barrier heights.[56,57] The HTBH38/04 set includes the forward and reverse barrier heights for 19 hydrogen transfer reactions, and NTBH38/04 consists of 19 nonhydrogen-transfer reactions.[57] We take the best theoretical estimates of the barrier heights and the geometries of all species from Ref. 57. From Table III, we see that LSDA substantially underestimates barrier heights. LC-ωLSDA and especially LRS-ωLSDA improve upon LSDA.

TABLE IV. Deviations from experiment of IPs and EAs computed using the uncontracted 6-311++G($3df,3pd$) basis set. All values are in eV.

	IP		EA	
Functional	ME	MAE	ME	MAE
LSDA	0.046	0.235	0.237	0.246
LC-ωLSDA	0.633	0.635	0.392	0.407
LRS-ωLSDA	0.028	0.195	0.189	0.192

Table IV presents the results for ionization potentials (IPs) and electronic affinities (EAs) in the G2 test set.[54] We dropped the ions H_2S^+, O_2^+, NO^-, and N_2^+ from this set again because of convergence issues with LSDA. In total, we used here 83 IPs and 57 EAs. LRS-ωLSDA performs much better than either LSDA or LC-ωLSDA. Global hybrids such as the popular B3LYP functional yield somewhat better MAE for IP (0.184 eV) and EA (0.124 eV).[55] Surprisingly, the results with LC-ωLSDA are particularly poor. We have repeated the LC-ωLSDA calculations self-consistently (instead of using LSDA orbitals), and the results are only slightly better than the post-LSDA results.

IV. CONCLUSIONS

Range-separated hybrids represent a new generation of density functionals that screen HF exchange. We have developed a novel LRS approach that uses a position-dependent screening function with an improved high-density scaling behavior. The current implementation uses a rather accurate approximation for the screened HF exchange energy density. LRS-ωLSDA has just one empirical parameter, fitted to experimental heats of formation. The results presented here indicate substantial improvement upon LSDA and LC-ωLSDA. More extensive studies of LRS are currently under way including its self-consistent implementation which is required for evaluation of analytic energy gradients and other properties.[58]

ACKNOWLEDGMENTS

This work was supported by the National Science Foundation (Grant Nos. CHE-0807194 and DMR-0501588) and the Welch Foundation (C-0036). We thank Dr. Ben Janesko and Dr. Tom Henderson for useful comments.

APPENDIX A: HIGH-DENSITY LIMIT FOR THE RANGE SEPARATION FUNCTION

Consider uniform density scaling[59] to the high-density limit:

$$\rho(\mathbf{r}) \to \rho_\lambda(\mathbf{r}) = \lambda^3 \rho(\lambda \mathbf{r}) \text{ and } \lambda \to \infty. \quad \text{(A1)}$$

The scaled density $\rho_\lambda(\mathbf{r})$ has the same number of electrons as $\rho(\mathbf{r})$ but is higher at the origin and more contracted around it. In this limit, in the absence of exact degeneracy of the Kohn–Sham noninteracting ground state, the exact exchange energy E_x^{ex} should emerge[60] to dominate E_{xc}:

$$\lim_{\lambda\to\infty} E_{\text{xc}}[\rho_\lambda]/E_x^{\text{ex}}[\rho_\lambda] = 1. \quad \text{(A2)}$$

Equation (A2) is an exact constraint on $E_{\text{xc}}[\rho]$ which can be satisfied by a hypergeneralized approximation[41,47,61] or by a locally range-separated hybrid. With a universal position-independent parameter ω in Eq. (2), however, it is incorrectly LSDA exchange that emerges instead:

$$\lim_{\lambda\to\infty} E_{\text{xc}}[\rho_\lambda]/E_x^{\text{LSDA}}[\rho_\lambda] = 1. \quad \text{(A3)}$$

Certainly there is no reason to believe that relative corrections to the local density approximation should vanish in the high-density limit.

To achieve the correct behavior of Eq. (A2), we need $\omega(\mathbf{r})$ to scale up faster than $\lambda\omega(\lambda\mathbf{r})$. Because $s(\mathbf{r}) \to s(\lambda\mathbf{r})$ and $r_s(\mathbf{r}) \to \lambda^{-1} r_s(\lambda\mathbf{r})$, Eq. (3) scales up like $\lambda\omega(\lambda\mathbf{r})$, which is much more nearly correct than is an ω that does not change under scaling.

Note that uniform density scaling relations for LR and SR exchange are presented in Ref. 62.

APPENDIX B: INVARIANCE OF LRS ENERGY WITH RESPECT TO INTERCHANGE OF ELECTRONS

We can write the exact exchange-correlation energy as

$$E_{\text{xc}} = \frac{1}{2}\int\int \frac{f(\mathbf{r},\mathbf{r}')}{|\mathbf{r}-\mathbf{r}'|} d\mathbf{r} d\mathbf{r}', \quad \text{where } f(\mathbf{r}',\mathbf{r}) = f(\mathbf{r},\mathbf{r}'). \quad \text{(B1)}$$

Suppose we have an approximation $f_{\text{approx}}(\mathbf{r},\mathbf{r}')$ that does not have the exact symmetry property. We can define a symmetrized

$$f_{\text{approx,symm}}(\mathbf{r},\mathbf{r}') = \tfrac{1}{2}(f_{\text{approx}}(\mathbf{r},\mathbf{r}') + f_{\text{approx}}(\mathbf{r}',\mathbf{r})), \quad \text{(B2)}$$

that has exactly the same energy integral as $f_{\text{approx}}(\mathbf{r},\mathbf{r}')$.

APPENDIX C: ANALYTIC INTEGRATION OF LRS HF EXCHANGE ENERGY DENSITY

Let $e^{-\alpha|\mathbf{r}-\mathbf{R}_1|^2}$ be an s-type Cartesian Gaussian function centered at $\mathbf{R}_1$ with orbital exponent α. Evaluating Eq. (7) with Gaussian basis sets requires the calculation of the following integral:

$$V^{\text{LR}}(\mathbf{r},\omega(\mathbf{r})) = \int e^{-\alpha|\mathbf{r}'-\mathbf{R}_1|^2} e^{-\beta|\mathbf{r}'-\mathbf{R}_2|^2} \frac{\text{erf}[\omega(\mathbf{r})|\mathbf{r}'-\mathbf{r}|]}{|\mathbf{r}'-\mathbf{r}|} d\mathbf{r}'. \quad \text{(C1)}$$

Using the Gaussian product rule,[63] we can rewrite Eq. (C1) as

$$V^{\text{LR}}(\mathbf{r},\omega(\mathbf{r})) = \int \tilde{K} e^{-p|\mathbf{r}-\mathbf{R_P}|^2} \frac{\text{erf}[\omega(\mathbf{r})|\mathbf{r}'-\mathbf{r}|]}{|\mathbf{r}'-\mathbf{r}|} d\mathbf{r}' \quad \text{(C2)}$$

where the exponent of the new Gaussian is $p=\alpha+\beta$, its center is $\mathbf{R_P}=(\alpha\mathbf{R_1}+\beta\mathbf{R_2})/(\alpha+\beta)$, and

$$\tilde{K} = e^{-(\alpha\beta/(\alpha+\beta))|\mathbf{R}_1-\mathbf{R}_2|^2}. \quad \text{(C3)}$$

The Fourier transform of the SR potential is

$$\frac{\text{erf}(\omega|\mathbf{r}-\mathbf{r}'|)}{|\mathbf{r}-\mathbf{r}'|} = (2\pi)^{-3}\int \frac{4\pi}{k^2} e^{-(k^2/4\omega^2)} e^{i\mathbf{k}\cdot(|\mathbf{r}-\mathbf{r}'|)} d\mathbf{k}. \quad \text{(C4)}$$

Using Eq. (C4) and substituting $1/q^2 = 1/p^2 + 1/\omega^2$, we can rewrite Eq. (C2) as

$$V^{\text{LR}}(\mathbf{r},\omega(\mathbf{r})) = (2\pi)^{-3}\tilde{K}\int \left(\frac{\pi}{p}\right)^{3/2} \frac{4\pi}{k^2} e^{-(k^2/4q^2)} e^{i\mathbf{k}\cdot\mathbf{r}} d\mathbf{k}. \quad \text{(C5)}$$

It is shown, e.g., in Ref. 63 that the integral in Eq. (C5) can be obtained analytically, so that

$$V^{\text{LR}}(\mathbf{r},\omega(\mathbf{r})) = \tilde{K}\left(\frac{\pi}{\alpha+\beta}\right)^{3/2} \frac{\text{erf}(q|\mathbf{r}-\mathbf{R_P}|)}{|\mathbf{r}-\mathbf{R_P}|}. \quad \text{(C6)}$$

[1] D. Pines, *Elementary Excitations in Solids* (Perseus Books, Reading, MA, 1999).
[2] G. Onida, L. Reining, and A. Rubio, Rev. Mod. Phys. **74**, 601 (2002).
[3] D. M. Bylander and L. Kleinman, Phys. Rev. B **41**, 7868 (1990).
[4] A. Seidl, A. Görling, P. Vögl, J. A. Majewski, and M. Levy, Phys. Rev. B **53**, 3764 (1996).
[5] H. Stoll and A. Savin, *Density Functional Methods in Physics* (Plenum, New York, 1985), p. 177.
[6] H.-J. Flad and A. Savin, Int. J. Quantum Chem. **56**, 327 (1995).
[7] A. Savin, in *Recent Developments and Applications of Modern Density Functional Theory* (Elsevier, B. V., New York, 1996).
[8] H. Iikura, T. Tsuneda, T. Yanai, and K. Hirao, J. Chem. Phys. **115**, 3540 (2001).
[9] O. A. Vydrov, J. Heyd, A. V. Krukau, and G. E. Scuseria, J. Chem. Phys. **125**, 074106 (2006).
[10] T. Leininger, H. Stoll, H.-J. Werner, and A. Savin, Chem. Phys. Lett. **275**, 151 (1997).
[11] O. A. Vydrov and G. E. Scuseria, J. Chem. Phys. **125**, 234109 (2006).
[12] O. A. Vydrov, G. E. Scuseria, and J. P. Perdew, J. Chem. Phys. **126**, 154109 (2007).
[13] J. Heyd, G. E. Scuseria, and M. Ernzerhof, J. Chem. Phys. **118**, 8207 (2003); **124**, 219906(E) (2006).
[14] J. Heyd and G. E. Scuseria, J. Chem. Phys. **120**, 7274 (2004).
[15] A. V. Krukau, O. A. Vydrov, A. F. Izmaylov, and G. E. Scuseria, J. Chem. Phys. **125**, 224106 (2006).
[16] H. J. Monkhorst, Phys. Rev. B **20**, 1504 (1979).
[17] J. Delhalle and J.-L. Calais, Phys. Rev. B **35**, 9460 (1987).
[18] J. Heyd and G. E. Scuseria, J. Chem. Phys. **121**, 1187 (2004).
[19] J. Heyd, J. E. Peralta, G. E. Scuseria, and R. L. Martin, J. Chem. Phys. **123**, 174101 (2005).
[20] J. E. Peralta, J. Heyd, G. E. Scuseria, and R. L. Martin, Phys. Rev. B **74**, 073101 (2006).
[21] P. J. Hay, R. L. Martin, J. Uddin, and G. E. Scuseria, J. Chem. Phys. **125**, 034712 (2006).
[22] V. Barone, O. Hod, and G. E. Scuseria, Nano Lett. **6**, 2748 (2006).
[23] I. D. Prodan, G. E. Scuseria, and R. L. Martin, Phys. Rev. B **76**, 033101 (2007).
[24] T. M. Henderson, A. F. Izmaylov, G. E. Scuseria, and A. Savin, J. Chem. Phys. **125**, 234109 (2006).
[25] T. M. Henderson, A. F. Izmaylov, G. E. Scuseria, and A. Savin, J. Chem. Theory Comput. **4**, 1254 (2008).
[26] E. Livshits and R. Baer, Phys. Chem. Chem. Phys. **9**, 2932 (2007).
[27] R. Baer and D. Neuhauser, arXiv:0804.3145.
[28] G. L. Oliver and J. P. Perdew, Phys. Rev. A **20**, 397 (1979).

[29] I. C. Gerber and J. G. Ángyan, Chem. Phys. Lett. **415**, 100 (2005).
[30] J. Toulouse, F. Colonna, and A. Savin, J. Chem. Phys. **122**, 014110 (2005).
[31] R. Pollet, A. Savin, T. Leininger, and H. Stoll, J. Chem. Phys. **116**, 1250 (2002).
[32] P. M. W. Gill, R. D. Adamson, and J. A. Pople, Mol. Phys. **88**, 1005 (1996).
[33] J. Tao, V. N. Staroverov, G. E. Scuseria, and J. P. Perdew, Phys. Rev. A **77**, 012509 (2008).
[34] P. M. W. Gill and R. D. Adamson, Chem. Phys. Lett. **261**, 105 (1996).
[35] D. L. Strout and G. E. Scuseria, J. Chem. Phys. **102**, 8448 (1995).
[36] M. C. Strain, G. E. Scuseria, and M. J. Frisch, Science **271**, 51 (1996).
[37] F. D. Salla and A. Gorling, J. Chem. Phys. **115**, 5718 (2001).
[38] J. Jaramillo, M. Ernzerhof, and G. E. Scuseria, J. Chem. Phys. **118**, 1068 (2003).
[39] L. M. Constantin, J. P. Perdew, and J. Tao, Phys. Rev. B **73**, 205104 (2006).
[40] T. M. Henderson, B. G. Janesko, and G. E. Scuseria, J. Chem. Phys. **128**, 194105 (2008).
[41] J. P. Perdew and K. Schmidt, in *Density Functional Theory and Its Applications to Materials*, edited by V. E. Van Doren, K. Alsenoy, and P. Geerlings (American Institute of Physics, Melville, NY, 2001).
[42] M. J. Frisch, G. W. Trucks, H. B. Schlegel *et al.*, GAUSSIAN Development Version, Revision D.01, Gaussian, Inc., Pittsburgh, PA, 2003.
[43] J. P. Perdew and Y. Wang, Phys. Rev. B **45**, 13244 (1992).
[44] B. J. Lynch and D. G. Truhlar, J. Phys. Chem. A **107**, 8996 (2003); **108**, 1460(E) (2004).
[45] L. A. Curtiss, K. Raghavachari, P. C. Redfern, and J. A. Pople, J. Chem. Phys. **112**, 7374 (2000).
[46] J. Krieger, J. Chen, G. Iafrate, A. Savin, in *Electron Correlation and Material Properties* (Plenum, New York, 1999).
[47] J. P. Perdew, A. Ruzsinszky, G. Csonka, O. A. Vydrov, G. E. Scuseria, V. N. Staroverov, and J. Tao, Phys. Rev. A **76**, 040501(R) (2007).
[48] D. C. Langreth and M. J. Mehl, Phys. Rev. Lett. **47**, 446 (1981).
[49] G. Sperber, Int. J. Quantum Chem. **5**, 189 (1971).
[50] M. Kohout, A. Savin, and H. Preuss, J. Chem. Phys. **95**, 1928 (1991).
[51] M. Levy, J. P. Perdew, and V. Sahni, Phys. Rev. A **30**, 2745 (1984) and references therein.
[52] F. E. Jorge, E. V. R. de Castro, and A. B. F. da Silva, Chem. Phys. **216**, 317 (1997).
[53] S. J. Chakravorty, S. R. Gwaltney, E. R. Davidson, F. A. Parpia, and C. F. Fischer, Phys. Rev. A **47**, 3649 (1993).
[54] L. A. Curtiss, K. Raghavachari, P. C. Redfern, and J. A. Pople, J. Chem. Phys. **106**, 1063 (1997).
[55] V. N. Staroverov, G. E. Scuseria, J. Tao, and J. P. Perdew, J. Chem. Phys. **119**, 12129 (2003).
[56] Y. Zhao, B. J. Lynch, and D. G. Truhlar, J. Phys. Chem. A **108**, 2715 (2004).
[57] Y. Zhao, N. Gonzáles-Garcías, and D. G. Truhlar, J. Phys. Chem. A **109**, 2012 (2005).
[58] G. E. Scuseria and H. F. Schaefer, Chem. Phys. Lett. **146**, 23 (1988).
[59] M. Levy and J. Perdew, Phys. Rev. A **32**, 2010 (1985).
[60] M. Levy, Phys. Rev. A **43**, 4637 (1991).
[61] J. P. Perdew, V. N. Staroverov, J. Tao, and G. E. Scuseria (unpublished) http://arxiv.org/abs/0808.2523.
[62] J. Toulouse, P. Gori-Giorgi, and A. Savin, Int. J. Quantum Chem. **106**, 2026 (2006).
[63] A. Szabo and N. S. Ostlund, *Modern Quantum Chemistry*, 1st revised ed. (McGraw-Hill, New York, 1989).